Journal of
Marine Science and Engineering

Article

Variability in Anthropogenic Underwater Noise Due to Bathymetry and Sound Speed Characteristics

Svein Vagle [1,*], Rianna E. Burnham [1,*], Caitlin O'Neill [1] and Harald Yurk [2]

1 Institute of Ocean Sciences, Fisheries and Oceans Canada (DFO), Sidney, BC V8L 4B2, Canada; caitlin.oneill@dfo-mpo.gc.ca
2 Pacific Science Enterprise Centre, Fisheries and Oceans Canada (DFO), Vancouver, BC V7V 1H2, Canada; harald.yurk@dfo-mpo.gc.ca
* Correspondence: svein.vagle@dfo-mpo.gc.ca (S.V.); rianna.burnham@dfo-mpo.gc.ca (R.E.B.)

Abstract: Oceanic acoustic environments are dynamic, shaped by the spatiotemporal variability in transmission losses and sound propagation pathways of natural and human-derived noise sources. Here we used recordings of an experimental noise source combined with transmission loss modeling to investigate changes in the received levels of vessel noise over space and time as a result of natural water column variability. Recordings were made in the Juan de Fuca Strait, on the west coast of Vancouver Island, a biologically productive coastal region that hosts several cetacean species. Significant variability in noise levels was observed due to changing water masses, tied to seasonal temperature variation and, on a finer scale, tidal movements. Comparisons of interpreted received noise levels through the water column indicated that vessel noise recorded by bottom-stationed monitoring devices might not accurately represent those received by whales in near-surface waters. Vertical and temporal differences of 3–5 dB were commonly observed in both the recorded and modeled data. This has implications in estimating the success of noise mitigation measures, and our understanding of the change in sound fields experienced by target species for conservation.

Keywords: anthropogenic noise; passive acoustic monitoring; sound speed profiles; natural variability; ray tracing models; transmission losses; noise mitigation implications; cetacean conservation; experimental noise source; vessel noise source

check for updates

Citation: Vagle, S.; Burnham, R.E.; O'Neill, C.; Yurk, H. Variability in Anthropogenic Underwater Noise Due to Bathymetry and Sound Speed Characteristics. *J. Mar. Sci. Eng.* **2021**, *9*, 1047. https://doi.org/10.3390/jmse9101047

Academic Editor: Giuseppa Buscaino

Received: 11 August 2021
Accepted: 18 September 2021
Published: 23 September 2021

Publisher's Note: MDPI stays neutral with regard to jurisdictional claims in published maps and institutional affiliations.

Copyright: © 2021 by the authors. Licensee MDPI, Basel, Switzerland. This article is an open access article distributed under the terms and conditions of the Creative Commons Attribution (CC BY) license (https://creativecommons.org/licenses/by/4.0/).

1. Introduction

Anthropogenic underwater noise is considered a major stressor on coastal marine ecosystems [1]. Human-generated noise sources are increasing in their distribution and abundance, altering the oceans' acoustic landscape [2–8]. Ocean background noise levels are now several decibels above pre-industrial levels, precipitated in large part by the introduction of motorized commercial shipping. An 8–10 dB re 1 µPa increase at frequencies <300 Hz in some ocean basins since the 1960s can be attributed to an increase in the number and size of vessels. This trend is projected to continue [3,5,9–13]. In coastal marine environments an increase in more localized vessel operations such as recreational and commercial fishing as well as tug and tow operations may lead to an increase in noise levels in addition to noise emissions from large commercial vessels [14,15]. Other human activities such as shore construction (e.g., pile driving) and seismic survey operations may further increase overall noise levels.

There is a need to quantify the extent to which human-derived noise impacts oceanic sound fields, and growing pressure to address the acoustic additions from vessels in order to protect marine ecosystems. Noise models can highlight areas of particular concern, but are usually focused on the transits of larger commercial vessels. As expected, they show that shipping lanes impose persistent sonic patterns on the marine environment [1,16–18]. Smaller vessels, however, have limited consideration in these models. Their presence and impact, especially in coastal regions, is underestimated [1,19].

Anthropogenic noise additions can be of particular concern for cetaceans [20]. Whales, dolphins and porpoises rely on their acoustic sense for navigation, foraging and retaining conspecific contact. Anthropogenic noise can mask acoustic signals by reducing the audibility and limiting the propagation of the signals, thereby reducing the effectiveness of navigation or foraging success. Vessel noise has also been shown to cause physiological stress, alter hearing sensitivity, change diving patterns and initiate avoidance behaviors [21–26].

Efforts to reduce noise from vessels have been attempted in several settings, with mitigation targeted to specific species or important habitat areas [27–32]. The effectiveness of these measures is frequently assessed by passive acoustic monitoring (PAM) systems deployed on or near the sea floor. While continuous acoustic monitoring is the key for describing the overall change in ambient sound conditions at a given location, this may not accurately represent the variation in the acoustic environment horizontally across space or vertically through the water column as perceived by marine life. Variability in sound fields is typically discussed over seasonal to diel periods and in reference to the differing levels of abiotic, biotic and anthropogenic inputs. Spatial variation is usually in reference to the variability in noise levels between recorders across an array or in a network, wherein differences arise from dominant sound sources at these locations, as well as from the propagation conditions determined by the water column properties, changes in bathymetry, and seabed substrate. There remains a paucity in our understanding of how the acoustic environment can vary without changes to the noise inputs, but through changes in sound transmission of the same sources through space and time at various scales.

Sound transmissions differ depending on water depth, topographical variation, substrate, water properties and sea surface conditions [33–39]. Changes in water structure define how sound is propagated from the source to a receiver to form the underwater sound field [40]. Our lack of understanding of the existing variation limits our ability to fully characterize sound fields, as well as understand the sound levels received by an animal.

This shortcoming also limits the effectiveness of assessing noise mitigation measures. If mitigation efforts target specific species, the noise variation needs to be assessed in frequencies audible and relevant to the species (functional hearing range; [41]) while focusing on the depths that are utilized by the animals. A second caveat relates to the habitat, and the inherent natural variability in the soundscape therein. Any observed noise reduction measurement needs to account for the natural variation in ambient noise as well as how vessels contribute to the measured ambient noise. Therefore, to assess the potential change resulting from a mitigation measure we require an understanding of the emitted noise levels by the anthropogenic source, the area-specific sound propagation, how sound transmission varies in both horizontal and vertical space and with time, and finally the ambient noise variation.

Here, we start by assessing the natural variability in sound levels in recordings from a single bottom-mounted PAM system, by considering the influence of local water properties and variable acoustic transmission loss. Then, we examine the natural variability in received noise levels from an experimental source to better calibrate the effectiveness of conservation measures designed to reduce anthropogenic ambient noise. Using a modeling approach, we also take a more whale-centric approach to understanding these changes, whereby sound field measures recorded by bottom-stationed systems will be compared to those potentially experienced by whales at diving depths.

2. Materials and Methods

2.1. Study Area

The PAM system was deployed off of Sooke in the Juan de Fuca Strait, on the west coast of Vancouver Island, British Columbia, in approximately 163 m of water (48° 17.3842 N, 123° 39.2284 W, Figure 1). The sound field in this area is impacted by noise from commercial vessels transiting international shipping lanes to major ports in Vancouver, Victoria, Port

Angeles, Tacoma and Seattle [42,43]. Recreational vessels also commonly use the same area, particularly during the summer [43]. The area is also a foraging habitat for several cetacean species, including gray (*Eschrichtius robustus*), humpback (*Megaptera novaeangliae*) and killer whales (*Orcinus orca*), as well as harbour (*Phocena phocena*) and Dall's porpoises (*Phocoenoides dalli*) [44–47], and is part of the designated critical habitat for southern resident killer whales (SRKW, [48–50]). Operational measures, such as vessel slow-down, route displacement and exclusion zones have been applied to this area and have reduced noise in frequencies used by SRKW for communication and echolocation [30–32,51].

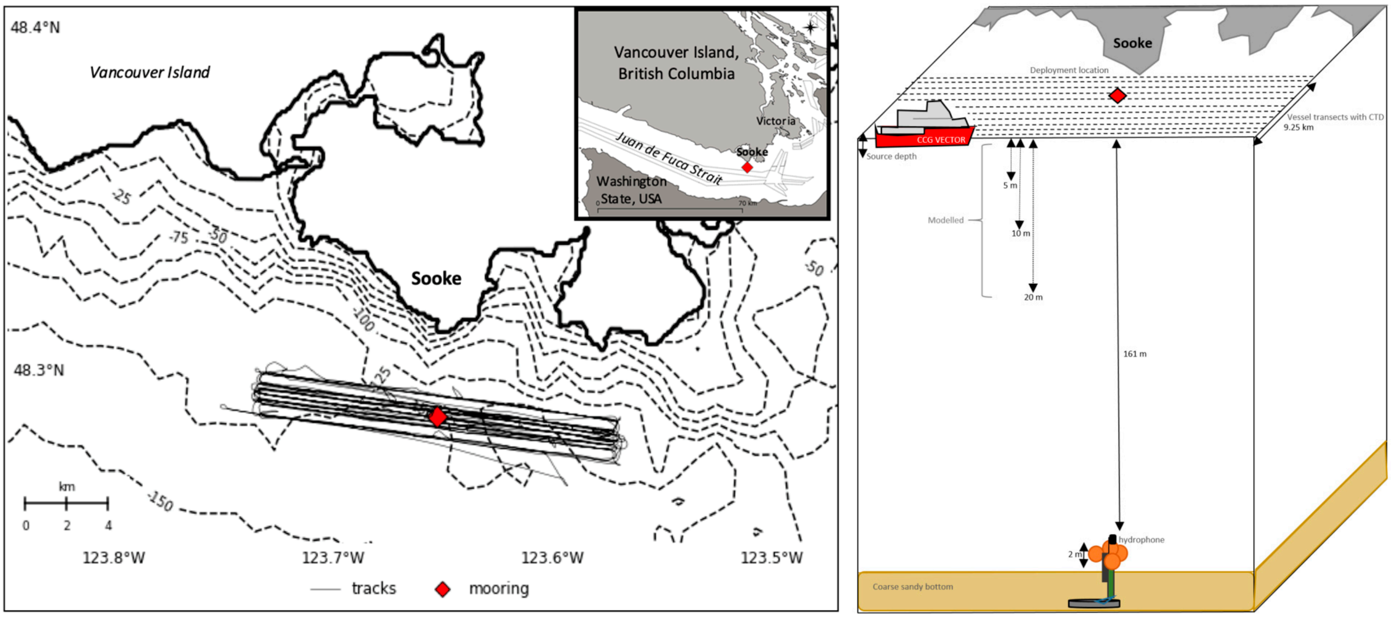

Figure 1. (**a**) Passive acoustic mooring location at Sooke in the Juan de Fuca Strait and vessel transects of the CCGS Vector, completed between 12–14 October 2018 to a maximum distance of 9.25 km from the mooring. Location of shipping lanes through the Juan de Fuca Strait are indicated by dashed lines in the inset. Depth contours in meters. (**b**) A schematic sectional plan of the experiment design showing the hydrophone at 161 m for observed measures and the interpolated assessments of the sound field at 5 m, 10 m and 20 m.

2.2. Acoustic Data Collection

Passive acoustic recordings were made from a calibrated Autonomous Multichannel Acoustic Recorder (JASCO AMAR-G4) equipped with a calibrated omnidirectional GeoSpectrum Technologies Inc. M36-100 hydrophone, sampling at 256 kHz with 24-bit resolution. The system was mounted onto a quiet mooring which positioned the hydrophone approximately 2 m off the bottom (Figure 1b). This mooring has been deployed in this location since February 2018, making continuous recordings and maintained through a regular servicing schedule (2–3 months). Here, we focused on the recordings made between services on 12 October and 29 November, 2018, wherein transects of an experimental noise source were completed immediately post-deployment in October. The acoustic data were stored on internal solid-state flash memory cards as uncompressed wav files. Upon retrieval of the mooring, the data were downloaded and the files post-processed using custom Python scripts (modified from [52]), using a 1-s Hanning window with 50% overlap and Welch's averaging to generate 1-min power spectral density (PSD) data in 1 Hz bands in the frequency domain. Noise levels in the sound field in the frequency range 100 Hz to 100 kHz were considered.

2.3. Experimental Noise Source

The research vessel used to deploy the mooring was also used as an experimental noise source during this experiment. The CCGS Vector is a coastal oceanographic vessel, with an overall length of 39.7 m, a beam of 9.5 m, a draft of 3.5 m and a total displacement of 560 tons. Cruising speed was approximately 10 knots (5.1 m s^{-1}) at 1500 RPM from a single three-bladed, variable pitch propeller driven by a 600 kW diesel engine [53]. The CCGS Vector was equipped with an AIRMAR Technology Corp. CM265LH Chirp-Ready sonar with an acoustic transducer (100 mm by 164 mm) operating at 50 kHz for navigational purposes and a 12 kHz SIMRAD 830-107783 sonar system with a 580 mm transducer used to detect water column depth for scientific operations. The nominal 3 dB power beam-down widths for these two systems are 21 degrees and 13 degrees at 50 kHz and 12 kHz, respectively. The CCGS Vector ran parallel transect lines from 22:00 12 Octoberto 06:00 14 October (UTC), 2018, from the deployment location increasing incrementally to approximately 9.25 km, with several repetitions made for each distance (Figure 1).

Most vessel-derived noise generated by a ship's propellers and machinery originate in the upper 10 m of the water column. The effective depth of the point source representation of the CCGS Vector was calculated from Lloyd's mirror (LM) effects during direct passage over the mooring (Figure 1). The LM effect, observed as a range-dependent alternation of peaks and nulls in frequency range spectrograms [54], results from interference created by the combination of direct and surface-reflected acoustic pathways. The depth of a noise point source, d_0, and receiver depth, d_1, were derived from the first two peaks, f_{p1} and f_{p2} [55], of the LM as:

$$f_{p1} = C_w \ r/(4d_0d_1) \text{ and } f_{p2} = 3 \times f_{p1} \quad (1)$$

where C_w = 1482 ms^{-1} and r is the slant range between the vessel source and the receiving hydrophone.

2.4. Sound Speed Profiles (SPP)

Profiles of conductivity and temperature as a function of depth (CTD) were obtained every two hours along the transects during the experimental noise exposure (12–14 October 2018) using a calibrated Seabird Scientific SBE-25 CTD. Salinity measures were derived from measured conductivity. Sound speed as a function of depth was then calculated from these data using the equations from [56]. These measures were augmented with synthesized data from the SalishSeaCast NEMO model [57,58]. Hourly data were downloaded from the SalishSeaCast model EDDAP server at a 400 m by 200 m spatial resolution from November 2017 to October 2018 (http://salishsea.eos.ubc.ca/erddap/ accessed on 30 March 2019, from the dataset ubcSSg3DTracerFields1hV18-06). These observed and modeled water properties were used to model the transmission loss variability over a year, running 1 November 2017, to 31 October 2018. Changes over time were examined using median values taken every six hours and monthly.

2.5. Transmission Loss and Sound Propagation Modeling

The sound spectral levels (SSL) of the CCGS Vector were calculated from the measured sound pressure levels (SPL, Figure 2) received at the acoustic mooring from direct overhead passes and for locations along transect lines at specific distances from the mooring, determined by comparing vessel GPS locations with the mooring location. To minimize variability in the vessel source spectrum and possible interference from other nearby vessels in the soundscape measures, only points of closest approach (CPA, ~350 m horizontal range) when the vessel was operating at 1500 RPM were used in this analysis.

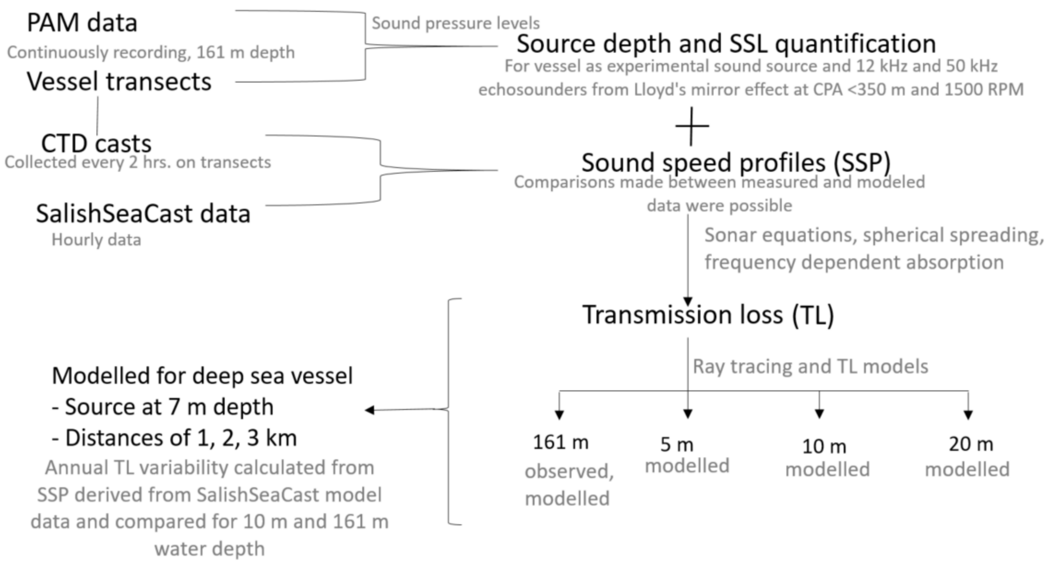

Figure 2. A flow diagram to demonstrate work plan and the integration of observed data and model results.

As a first step to investigate the natural variability in propagation characteristics, spherical spreading was assumed together with frequency-dependent absorption, α(f) (dB/m, [59]), resulting in a sonar equation of the form:

$$\mathrm{SSL(f)} = \mathrm{SPL(f)} + 20 \times \log10(\mathrm{r}) + \alpha(\mathrm{f}) \times \mathrm{r} \quad (2)$$

where r is the slant range between the source and the receiver, and α(f) was applied for frequencies, f, between 200 Hz to 100 kHz as derived by Francois and Garrison [59]. Using these assumptions, source levels of the CCGS Vector were derived and then expressed as median and quartile (25th and 75th) values for each third-octave band.

Variable transmission loss resulting from the sound speed profile field was modeled (Figure 2) using two-dimensional propagation models accounting for range and depth. For propagation of acoustic frequencies above 1 kHz a model based on ray theory was used [60,61], modified to include absorption loss by sediment and frequency dependent absorption by ocean water [59]. The accuracy in the wave equation for a receiver depth of 2 m would be compromised below 400 Hz [62]; therefore, for frequencies between 10 and 1000 Hz, a widely used range-dependent acoustic model (GeoRAM), based on the U.S. Navy's standard split-step Fourier parabolic Equation (PE) model was used [63,64]. The models were run using the measured sound speed profiles from the CTD casts at the mooring location, as well as sound speed profiles derived from the SalishSeaCast model, and tidal timing as well as elevation data obtained from the WebTide model [65]. These calculated profiles and high-resolution bathymetry data were used to form depth-dependent transmission loss estimates at distances extending from the mooring location to the outbound shipping lane (~3 km, Figures 1 and 2). Estimates were made at 1 km increments to this maximum, to represent received noise from a deep-sea vessel in the shipping lane. Transmission loss was also calculated for surface (5 m), upper to mid-water column (10 m and 20 m) and hydrophone depths (161 m). The upper water column depth of 5 m represents whales spending time in near-surface waters and during inter-ventilation dives. The 10 m and 20 m depths represent the depth of average swimming and foraging dives [66–71].

Sound propagation models appropriate for coastal waters quantify a sinusoidal wave of a specific frequency, with a frequency cut-off, f_c, determined by substrate material and water column depth. This is expressed as:

$$\mathrm{f}_c = \frac{c_w}{4H}\sqrt{1-(c_w)^2(c_s)^2} \quad (3)$$

where c_w is the speed of sound in the water column; c_s is the speed of sound in the sediment; and H is the water depth in the direction of the sound propagation [72]. We assumed the sediment of the study area to be coarse sand, based on samples collected by Haggarty et al. [73]. This is a general characterization that was used for ease of modeling, and perhaps does not take into account the finer scale variance and sediment transport seen in work of others [74,75]. Speed of sound c_s = 1800 m s^{-1} and sediment density ϱs = 2000 kg m^{-3} values were used [76,77]. Using these parameters and an average water column sound speed of c_w = 1482 m s^{-1}, the lower frequency cut-off for our experiment was approximated, to examine if the broadband frequency range of 10 Hz to 100 kHz was appropriate.

3. Results

3.1. Experimental Noise Source

Spectrograms of direct passes over and transits lateral to the mooring by the CCGS Vector showed significant noise generated at all frequencies between 100 Hz and 100 kHz (Figure 3). Recordings taken from the moorings showed noise additions from the CCGS Vector transects in the 1–10 kHz range to exceed 6 dB at distances 3 km or more in horizontal range (Figure 3). This focus area of 3 km is the distance between the mooring deployment location and the outbound shipping lane. In the low frequencies (<1 kHz), the detectable range was approximately 1 km, whereby the additions were not discernable from the background ambient noise field beyond this distance. A similar detection distance was found for noise in frequencies of 20 kHz and higher. The acoustic signature of the approach to and passing of the mooring by the CCGS Vector was asymmetric, with a greater noise field created following the passage of the vessel. The 12 kHz Simrad sonar was easily discerned at ranges exceeding 3 km, both when the vessel was approaching and leaving (Figure 4). Similarly, the 50 kHz navigational sonar was detected at a range of 1.5 km both ahead and behind the passing vessel (Figure 4).

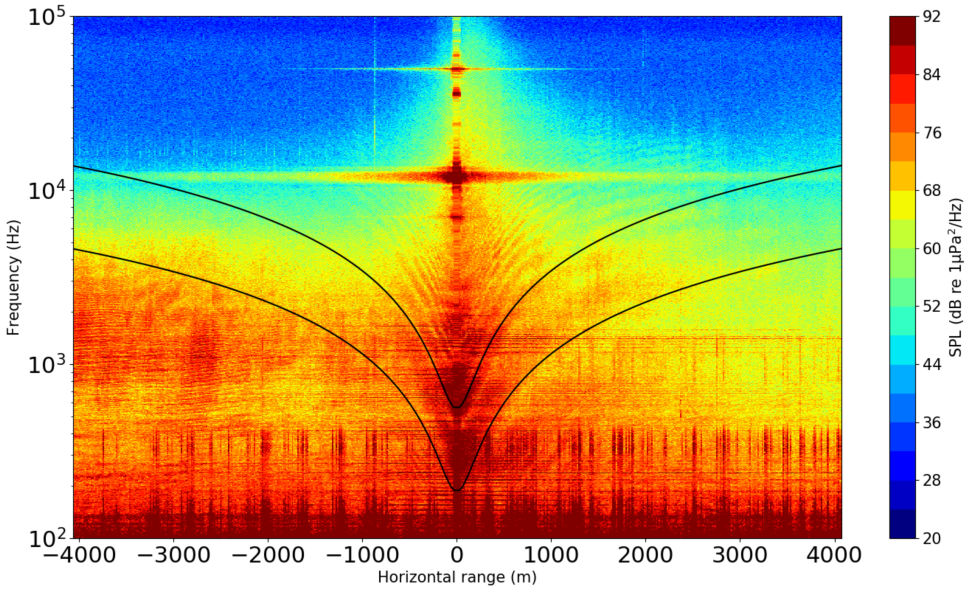

Figure 3. Spectrograms relative to the location of the PAM mooring for a transit of the CCGS Vector at a constant speed at 1500 RPM. The first two Lloyd's mirror effect peaks are highlighted with black lines. The vessel is travelling from left to right.

Using Equation (1), and assuming perfect reflection from the surface and disregarding refraction effects [55], the effective depth of the noise point source for the CCGS Vector was calculated from spectrograms of the LM effect (Figure 3), whereby the vessel source depth, d0, was 2 m and the receiver depth, d1, was 161 m. The SSL at 12 kHz and 50 kHz for the vessel sonars were estimated to be 154 and 159 dB re 1μPa^2, respectively (Figure 3). Spatial transmission losses for these active sonars were also estimated (Figure 4).

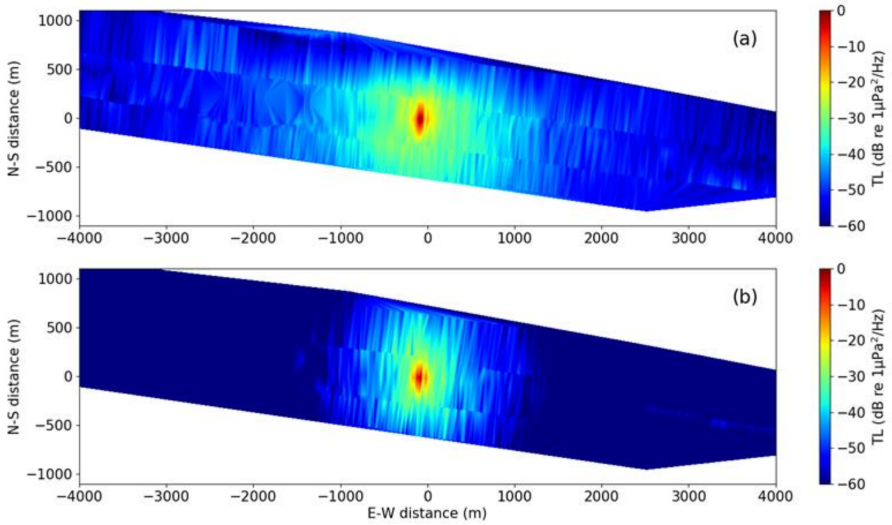

Figure 4. Spatial transmission loss for the two sonar systems on the CCGS Vector. Received sound pressure levels (SPL) relative to maximum SPL for the (**a**) 12 kHz and (**b**) 50 kHz sonars are shown.

3.2. Sound Speed Profiles

Sixteen sound speed profiles as a function of depth were obtained during the 36-h experimental transects using the CTD data (Figures 5 and 6). Modeled profiles from the SalishSeaCast model were compared to the observed measures (Figures 5 and 6), and both were then combined to generate hourly sound speed profiles used in transmission loss modeling for the transect period. Both the observed and modeled data suggest a change in water properties, and so sound speed profiles, at approximately 50 m and again between 100 and 150 m (Figures 5 and 6). These were most pronounced as the tidal flow changed direction (Figure 4). Differences between the modeled and observed profiles may be due to more localised wind and wave effects effecting sea conditions in a finer spatiotemporal resolution than the model predicts, and changes in model resolution with depth [57,58].

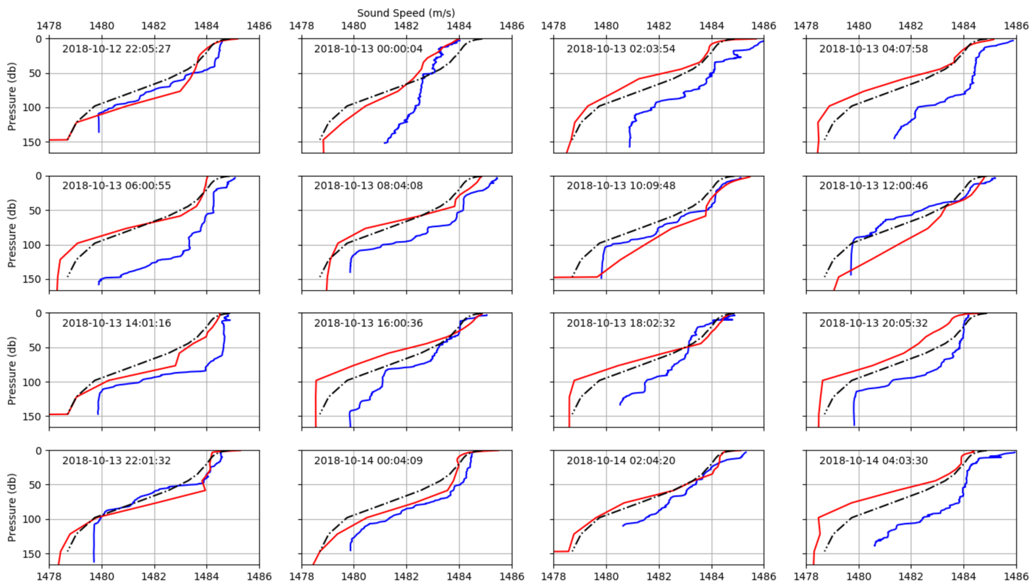

Figure 5. Sound speed profiles observed in the vicinity of the Sooke mooring at the UTC times indicated in each panel (blue lines), derived from CTD casts made on transects past the mooring between 22:00 12 October to 06:00 14 October (UTC), 2018. Also shown are sound speed profiles as obtained from the SalishSeaCast model at the nearest grid point and nearest time (red lines) to the measured data. The broken black lines show the average modeled sound speed profile for this period during the experimental source exposure.

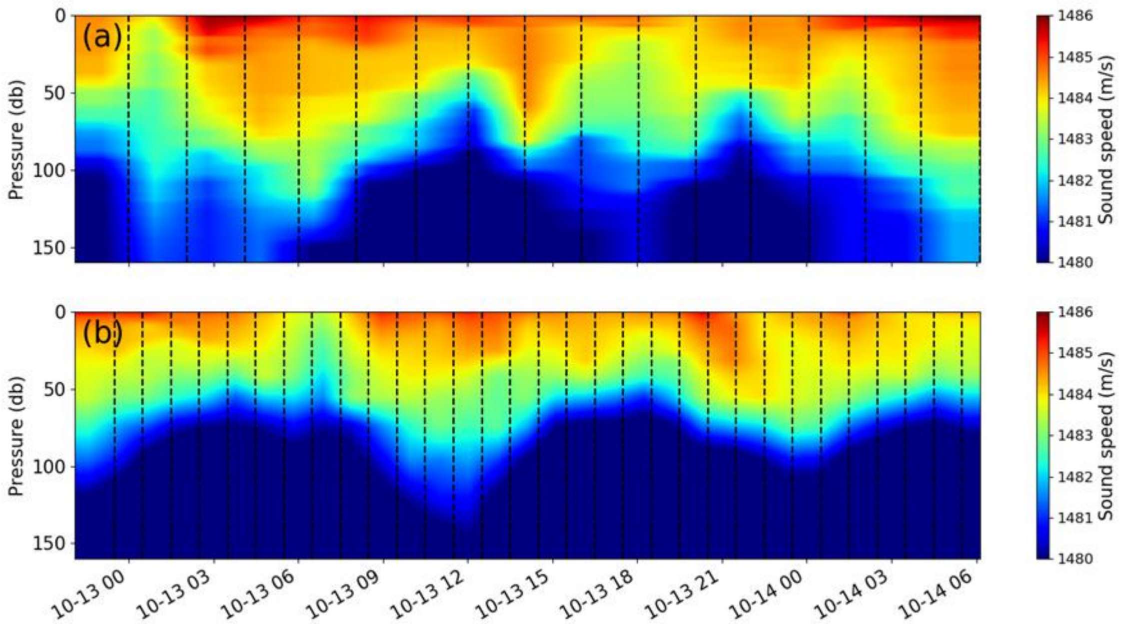

Figure 6. Comparison of the sound speed field as function of pressure for the period when the CCGS Vector was near the Sooke mooring. (**a**) Observed sound speed field and (**b**) the field obtained from the SalishSeaCast model data. The dashed lines indicate the times of the available profiles.

3.3. Transmission Loss and Sound Propagation Modeling

Variability in the received noise levels at times when the CCGS Vector was the major contributor (CPA < 350 m, travelling at 1500 RPM) was examined from thirteen instances over the 36-h test period. From these measured received levels, back-calculation using Equation (2) and frequency-dependent absorption and spherical spreading assumptions [59] were utilized to derive the median and quartile source level values for the CCGS Vector, showing interquartile ranges from 1.5 dB to 5 dB ($\overline{x}$ = 2.25 dB) (Figure 7). Assuming that the SL of the vessel remained constant for all CPA transects, the observed variability in calculated SL is an indication that the actual transmission losses did not correspond to the spherical losses assumed in Equation (2). Features in the 12.8 and 51.2 kHz third-octave bands were attributable to the active vessel sonars (Figure 7).

Using the ray tracing and GeoRAM transmission loss (TL) models forced by the combined measured and modeled sound speed profiles, a number of transmission loss metrics can be calculated to show the TL variability resulting from changing water properties and tides. Hourly departures from the median TL calculated at 10 kHz for a sound source at a depth of 2 m at a range of 3 km (outbound shipping lane) for noise received at four water depths (5, 10, 20 and 161 m) at the location of the PAM mooring were modeled (Figure 8). The near-surface (5 m) TL showed significant variability, reaching 10 dBs over the 36-h period, while the near-bottom (161 m) results indicate much less variability, in the 1 dB range (Figure 8b). The TL at 10 and 20 m depths show similar behaviors and variability, reaching $\pm$ 0.5 dB, with a possible correlation with tidal elevation (Figure 8a,c). The discrepancies between the TL observed near the sea floor and noise levels in the upper water column were taken into consideration by the difference in results from 161 m and 10 m (Figure 8d).

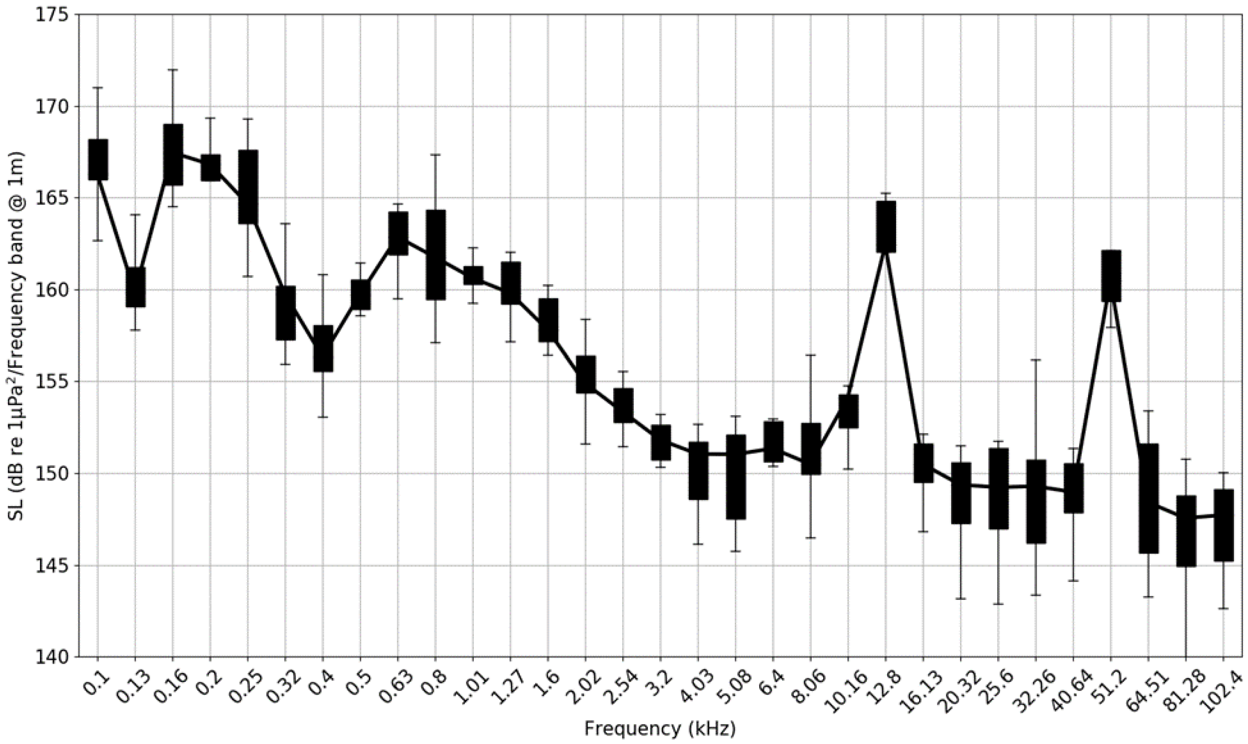

Figure 7. Box plot of third-octave band (center frequency of each band as indicated) calculated SLs for the CCGS Vector at the closest point of approach for 13 transects. In each box the solid horizontal line in the middle is the median (L_{50}) value, and the boxes are defined by L_{25} and L_{75}. The whiskers extend outside the boxes to the highest and lowest observations that fall within 1.5 times the interquartile range (IQR). The IQR is the range measured from the 25th to the 75th percentile (L_{25} to L_{75}).

Variability in the calculated TL values due to seasonal changes in the sound speed field was examined by running the TL models at 10 kHz using the hourly sound speed field over the year of data extracted from the SalishSeaCast model. The results were expressed as TL relative to the median values as a function of depth and time. These were then applied to an example for a deep-sea vessel with the noise source modeled at a depth of 7 m at distances of 1 km, 2 km and 3 km south of the mooring over a 12-month period (1 November 2017–31 October 2018, Figure 9). This would allow for comparison from our experimental source results to the deep-sea commercial vessel traffic prevalent in the study area, and a source of acoustic disturbance of concern for the marine species foraging in the Salish Sea.

The sound speeds derived from the SalishSeaCast model were generally lowest near the surface in the cooler waters from November 2017 to mid-July 2018, but increased with depth, with fluctuations due to changes in water properties (Figure 9a). Transmission loss was generally greatest in the upper 10 m and decreased with depth during this winter period. However, as the vessel mooring distance was increased in the model, so did the variability in TL in deeper layers, and at times the TL at 60–80 m depth equaled those seen in the surface layer (Figure 9d). During the summer and fall months (August to November) the sound speed increased significantly in the upper 50 m as a result of temperature stratification (Figure 9a). The resulting effect on TL was a significant increase in both depth and source–receiver distance (Figure 9b–d). In the upper waters, TL for a source at 1 km was reduced, while TL significantly increased for a source at 3 km. For source–receiver distances modeled at 2 and 3 km for this deep-sea vessel example, water layers below 100 m experienced reduced TL during this period. Overall, the variability in TL relative to the 12-month median values ranged between −3 and +3 dBs. The seasonal and depth variability of the modeled TL (Figure 9) were emphasized by extracting selected receiver depths (Figure 10, shown for depths of 10 and 161 m, corresponding to upper water conditions and the location of the PAM mooring) as we did before. The received variability is significantly greater in the upper layer during all months, while at greater depth variability is minimal during the winter and spring months. Some periods of significantly reduced TL at greater depth were seen during the summer. This suggests that whales using the Strait of Juan de Fuca and waters coastward of the outbound shipping lane, to transit or forage during the summer, would be subject to greater commercial vessel noise in the lower water column.

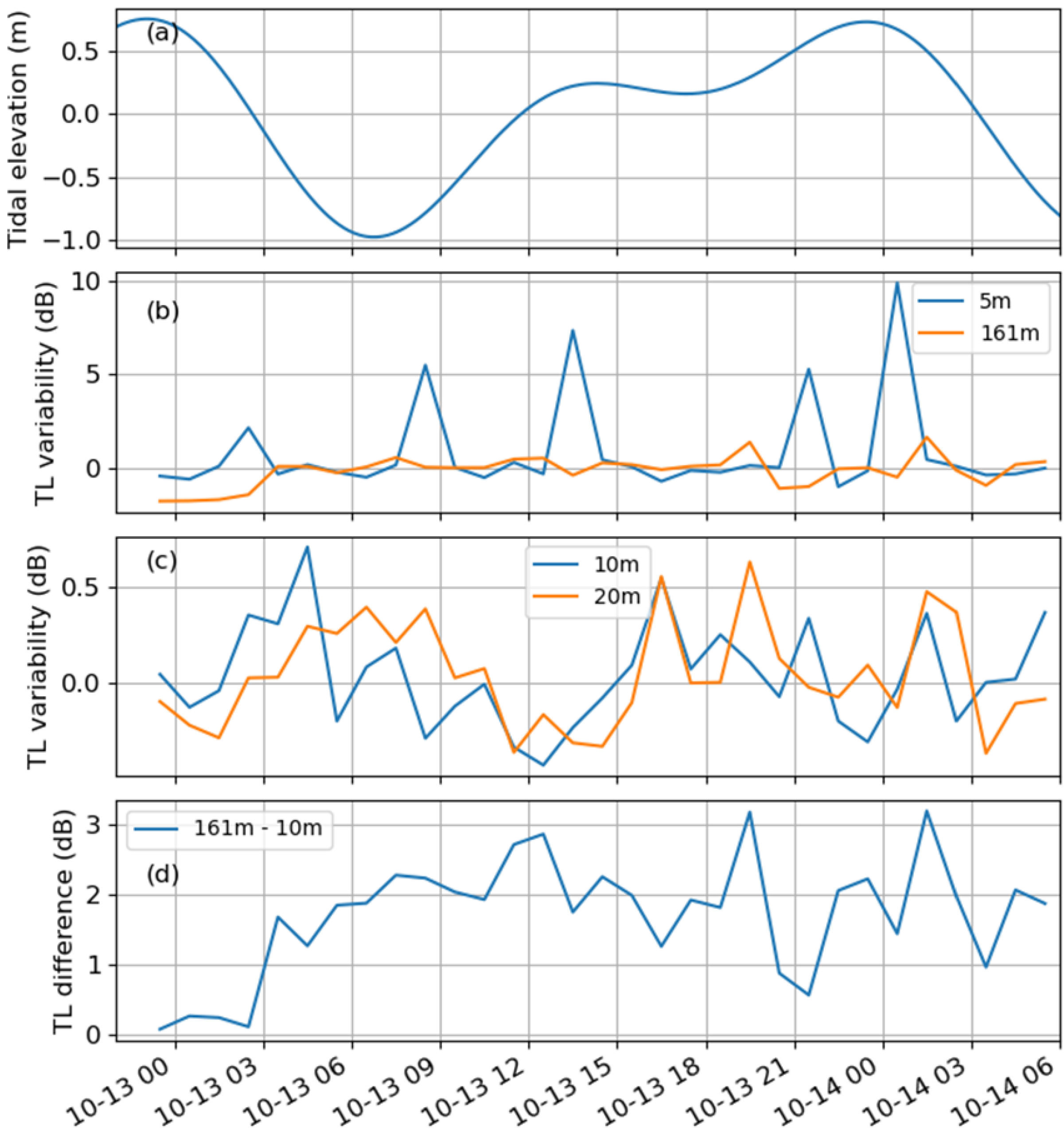

Figure 8. Tidal elevation at the Sooke mooring (**a**); modeled transmission loss (TL) variability at different depths (**b**,**c**); and the TL difference from modeled values between 161 m and 10 m depths (**d**). The acoustic frequency modeled was 10 kHz and the source depth was 2 m at a range of 3000 m south of the mooring location, in the middle of the outbound shipping lane.

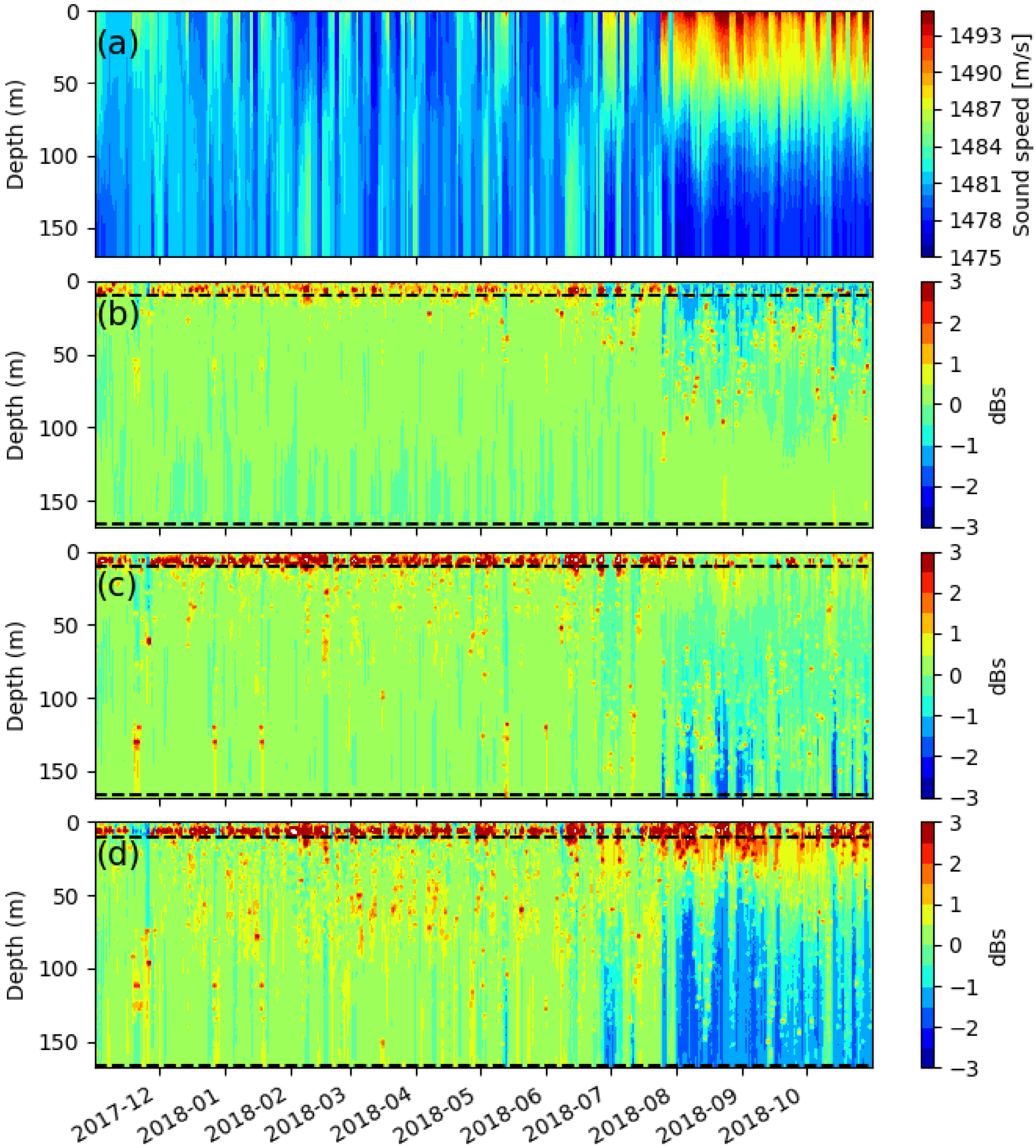

Figure 9. (**a**) SalishSeaCast-model-derived sound speed profiles; (**b**) six hourly modeled TL minus the 12-month median values when the source-to-receiver distance was 1000 m; (**c**) same for when the distance was 2000 m; and (**d**) when the distance was 3000 m. The dashed horizontal lines indicate the depths of 10 m and 161 m from which the TL variabilities are shown in Figure 10.

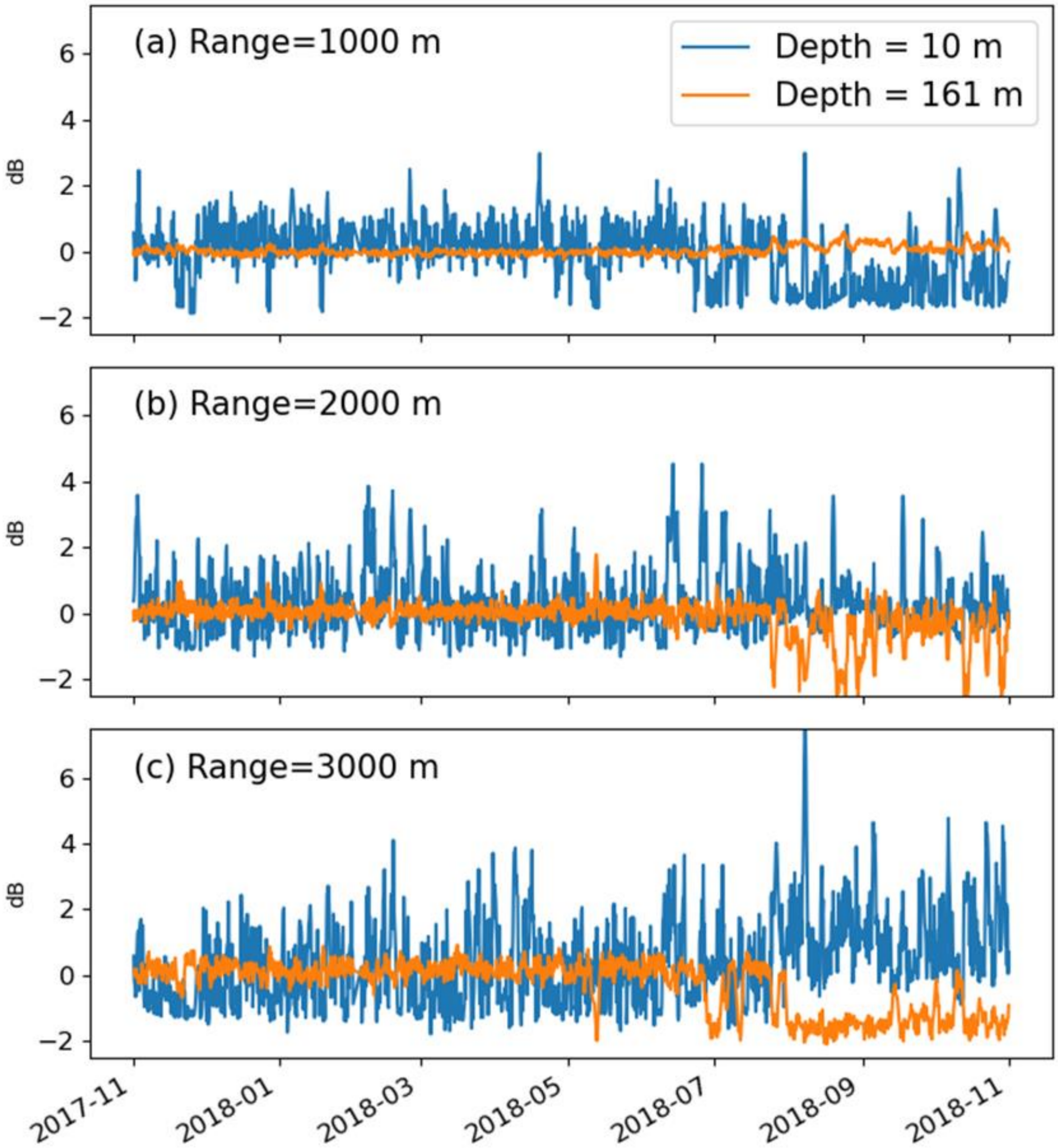

Figure 10. Departures from the annual median of the modeled TL for two depths: 10 and 161 m, corresponding to typical dive depths of SRKW and the location of the PAM mooring, respectively. Results taken from modeled TL for source receiver ranges of (**a**) 1000 m, (**b**) 2000 m and (**c**) 3000 m, and a source depth of 7 m, representing a commercial deep-sea vessel.

4. Discussion

Characterization of acoustic environments and the inputs from human-derived noise on different spatial and temporal scales is required to improve our understanding of the impacts of noise emitted into oceanic sound fields. For this analysis, we used the CCGS Vector as an experimental noise source in a case study of sound propagation and noise variability from anthropogenic sound sources in a highly biologically productive coastal region. The calculated SPL and LM effect spectrograms showed significant noise additions in the broadband frequency range of 100 Hz to 100 kHz. They also showed an asymmetry in received acoustic energy as the vessel passed and moved away from the acoustic mooring, likely due to the shadowing effect of the hull in the forward direction [53], indicating that the acoustic disturbance outlasted the physical presence of the vessel.

The transmission loss modeling showed significant spatial and temporal variability in received noise levels on several scales. The results indicate substantial short-term variability over space (both vertical and horizontal) and over time; for our experimental noise source this was in the range of several decibels in just a few hours. Tidally driven changes in water masses influenced the local sound speed characteristics, resulting in natural variability dependent on the noise source and local sound speed field. Significant stratification of the noise transmission over depth and range was especially seen during the summer and fall (Figures 9 and 10). During this period, surface warming promoted greater sound speeds in the upper layers, which resulted in downward refraction of noise generated in these warmer waters. Generally, such conditions would suggest increased TL and therefore improved conditions for marine life using the upper part of the water column. Our results do show that this is indeed the case in certain circumstances. However, depending on the source–receiver distance (Figures 9 and 10) and the source depth (not shown), the TL can either be higher or lower relative to longer term median values. During the summer and fall period characterized by strong thermal stratification, the temporal- and depth-dependent variability in TL was considerable at this location. In the inner, more protected waters of the Salish Sea, where water mixing with colder Pacific waters is less prominent, it would be expected that the period with such warmer surface water conditions could be even longer. Although temperature was thought to be the greatest driver in changes in TL, especially seasonally, the influence of change in conductivity/salinity was also part of the sound speed profile calculations. Haloclines could strengthen the influence of thermoclines, formed from seasonal forcing of fresh, fluvial or more saline, deep oceanic waters [58]. Circulation driven by discharge of the Fraser River, modulated by the tide, forms the salinity structure of areas in the Juan de Fuca Strait and the Salish Sea more widely [58,74].

The noise propagation and variability analyses demonstrated the potential impact of vessels on the sound field. At greater depth, the acoustic environment would likely be dominated by acoustic additions from deep-sea vessels in the outbound traffic lane propagating over several kilometers.

This can impact the ability of cetaceans to communicate and forage. For threatened or at-risk cetacean species using this area, elevated noise levels may be pervasive, especially in areas critical to their survival [48,78,79]. The broadband nature of the noise from our experimental source and modeled deep-sea vessel example exposes the potential for masking communication and acoustic cues of the species frequenting the area. These broadband additions are in line with those described for transiting larger commercial vessels, which have been noted to produce noise in ranges of 125 Hz to 20 kHz [1,16–18,80]. Low-frequency noise would have the most impact on the baleen whale species whose functional hearing range is presumed to be in lower frequencies [41], whereas the additions in the higher frequencies have implications on the calling and echolocation abilities of killer whales, dolphins and porpoises. A 6 dB increase in noise contribution by the source vessel in the 1–10 kHz band at distances of up to 3 km represents a considerable impact on the communication range of endangered SRKW, whose communication signal energy is focused in this frequency band [81,82]. Due to the frequency-dependent propagation of acoustic signals, the propagation of the lower frequency components of calls determines the maximum distance over which killer whales can communicate. These lower frequency components are also at greater risk of being masked by ship noise. For SRKW, noise additions would impact social calls [83], used to maintain cohesion of tightly knit family groups [46,69,84]. Noise which limits the distances over which resident killer whales can communicate may not only affect their ability to socialize but also limit the extent of an area a group can explore for prey during foraging and cooperatively hunt within.

The comparison of sound transmission through the water column creates a more whale-centric appreciation of the sound field. Most whales typically spend more time in the upper to mid-water column where swimming and diving is more efficient [85]. In our study area, whales may experience elevated noise levels in the surface waters resulting from nearby vessels. This could impact the whales' ability to successfully locate and capture prey, and will limit the spatial extent over which they can actively and passively receive acoustic information used for navigation and social interactions. Increased sound propagation in the upper water column during the summer period when whales predominantly use these waters could affect the range over which the whales' signals can travel, and this may influence the noise masking of these signals depending on where the noise source is relative to the signaling and receiving animals. Furthermore, the surface sound duct observed in the upper water layers may bend echolocation clicks of the odontocete species upwards, potentially reducing the vertical range of the signals, i.e., reducing detection of prey at depth and limiting the ability to navigate. At the same time, distant shipping noise from large commercial vessels in the shipping lane may interfere with the pursuit of prey at depths in areas where the shipping lanes are close to foraging areas of the whales. The depth of the mooring (161 m) approximately replicates maximum diving depths for foraging SRKW [45,71,86], indicating that foraging at depth could still be hindered by vessel noise from more distant sources.

The asymmetry of the vessel noise LM signature in approach, compared to the more elevated additions after passage, may hinder an appropriate diving response from whales in proximity to vessels, and increase the likelihood of vessel strikes. This finding also has implications for the impact of whale watching on whales, whereby minimum approach distance, vessel maneuvering and speed of acceleration in the vicinity of whales may need greater consideration. The Government of Canada has implemented an Interim Order to protect SRKW under the Canada Shipping Act, but more guidelines may be needed for vessel etiquette while engaged in a whale encounter and after it has concluded.

Mitigation measures for vessel noise can be classified either as source-oriented, whereby vessel modification, retrofitting or re-design reduces cavitation and propeller noise outputs [87], or operational, which includes changes to vessel route, speed or timing. Vessel slowdown, displacement and exclusion have been successfully used in the study area to reduce vessel noise [30–32]. Received sound levels have decreased in the range of 0.5–3 dB/knot for commercial vessels reducing speed in shipping lanes, depending on the frequency range that is considered [42,88]. However, the results from the natural variability analysis have implications as to how we might understand outcomes from conservation measures targeted at reducing underwater noise for marine species.

The transmission loss estimates suggest that during the time of these operational measures (summer–fall) the natural variability in noise levels could be similar to the SPL reductions reported (0.5–4 dB). This variability was highest when changes were considered at a distance of 3 km, or approximately the distance of the outbound shipping lane from the mooring (Figures 9 and 10). Reducing the number of vessel transits has also been shown to reduce ambient noise levels, whereby median SPL in vessel exclusion areas have shown reductions greater than the estimated natural variability in sound field measures, particularly when the numbers of smaller recreational vessels were limited [32]. However, a reduction in commercial vessel traffic by approximately 13–16% through the Salish Sea only reduced weekly median power spectral density, at most, by 5.8 dB, with this estimate subject to large variability [89]. This suggests that large-scale changes in commercial traffic would be needed to create reductions in ambient noise levels that significantly exceeded those resulting from natural change. However, it is worth noting that median SPL has been shown to be an inappropriate metric to measure short-term variation in noise levels and that at least three decades of continuous monitoring would be required to detect trends of similar magnitude to historic rises in noise levels observed in the Northeast Pacific [14]. A different or more stringent mitigation approach may be needed to include consideration of natural sound level variability. Permanent vessel no-go zones for smaller vessels combined with a reduction in frequency of large vessel passages, or re-routing shipping lanes within or outside of critical habitats [27,90], can increase the amount of time when threatened whale species are subjected to only natural ambient noise variation in critical habitats.

Noting the natural variability in the soundscape of an area also gives us an indication of the ability of the whales to compensate for higher noise levels and perhaps allows a better assessment of the impact of anthropogenic noise additions to the natural sound field. However, generalizing from calling modifications used to overcome natural noise to anthropogenic noise sources may not be appropriate due to differences in intensity and frequency of the noise [91]. Particularly, time integration of the measured noise signal has to match the auditory filter and critical bandwidth of the animal's auditory system, and there are still very few studies that target hearing abilities in free-ranging cetaceans [92,93]. Given the paucity of information available on cetacean hearing and the auditory impact of noise on whales in the wild, it may be useful to apply a cautionary approach and assume that a considerable reduction in human-derived noise is needed to achieve a significant relief from anthropogenic noise for marine mammals. Natural noise variability may point to adaptation to ambient noise in cetaceans; the level at which additional anthropogenic noise in particular frequencies may impact each species, however, is poorly understood.

The management of underwater noise pollution, particularly from vessels, is a pressing conservation issue for all marine life. Our analysis describes the variability in received noise levels from one experimental source and modeling from one particular location; however, the Salish Sea is well-utilized by small and large vessels. Recordings from the Juan de Fuca Strait indicate that vessel noise is consistently present [94]. As a trader in natural resources surrounded by oceans, Canada relies on oceanic transportation of goods. The current ship traffic density appears to produce noise levels that have detrimental impacts on at least some species and any increase in marine shipping, particularly through the Juan de Fuca Strait and the Salish Sea, could increase that impact [95]. To better identify the benefits resulting from anthropogenic noise mitigation measures, sound field examinations should include acoustic data describing the natural variability of ambient noise, because reductions in the anthropogenic part of the noise field could be seemingly elevated or masked by significant natural variability. Furthermore, we posit that future mitigation schemes should incorporate noise variability and transmission loss modeling, and that any mitigation measures need to respond to both long-term and wide-scale ambient noise increases, seasonal changes in sound propagation pathways, and fine-scale temporal and spatial variability in noise transmission. The work presented here also acknowledges that noise is not uniformly sourced in the oceans, and that bottom-stationed acoustic moorings may not best represent the sound field experienced by marine species transiting or foraging in an area. Whales utilize specific water depths particular to their biology and functional use of the area, and respond to the presence of prey in the water column as well as the spatial and temporal variation in prey abundance. Spatial and temporal changes in ambient noise, both vertically and horizontally, affect the ability of cetaceans to send, receive and interpret acoustic signals, and the animals may make decisions of where and when to forage based on the noise levels.

Our work suggests that to fully understand the implications of human-derived noise on sound fields, as well as mitigation measures put in place to lessen their effects, it is necessary to consider the natural variability resulting from seasonal and tidally driven changes in sound propagation. Our results suggest that cetaceans using the coastal waters of the Juan de Fuca Strait in the summer will have greater vessel noise inputs while in the lower water column. For endangered SRKW these represent depths where they may pursue and catch prey. Measures in place to reduce acoustic disturbance from commercial traffic at this time may be less effective during deep-water dives in the summer months. We suggest that to estimate the efficacy of measures for target species, reduction in noise levels in frequencies and at depths relevant to these species should be assessed. More work is needed to characterize the human-derived noise in soundscapes, as is also the case for whale habitat use and diving behavior, in order to increase the efficacy of protective measures implemented in coastal regions for cetaceans.

Author Contributions: Conceptualization, S.V., R.E.B. and H.Y.; Methodology, S.V. and R.E.B.; Validation, S.V. and R.E.B.; Formal Analysis, S.V. and R.E.B.; Investigation, S.V. and R.E.B.; Data Curation, C.O.; Writing—Original Draft Preparation, S.V. and R.E.B.; Writing—Review and Editing, H.Y. and C.O.; Visualization, S.V. and R.E.B.; Supervision, S.V.; Project Administration, S.V. and C.O. All authors have read and agreed to the published version of the manuscript.

Funding: This work is part of an ongoing program of the Government of Canada, and was funded by the Ocean Protection Plan–Marine Environmental Quality Program (OPP/MEQ).

Institutional Review Board Statement: Not applicable for this study.

Informed Consent Statement: Not applicable for this study.

Data Availability Statement: The data presented in this study are available on request from the corresponding author. The data are not publicly available due to being part of ongoing work.

Acknowledgments: The officers and crew on the CCGS Vector for all their help with servicing our hydrophone moorings in the Salish Sea. The members of our field crew that collected the CTD data (Scott Rose, Hugh Maclean, Cynthia Wright and Mark Belton). Christie Morrison for helping with Figure 1.

Conflicts of Interest: The authors declare no conflict of interest.

References

1. Erbe, C.; MacGillivray, A.; Williams, R. Mapping cumulative noise from shipping to inform marine spatial planning. *J. Acoust. Soc. Am.* **2012**, *132*, EL423–EL428. [CrossRef]
2. Richardson, W.J.; Greene, C.R., Jr.; Malme, C.I.; Thomson, D. *Marine Mammals and Noise*; Academic Press: San Diego, CA, USA, 1995; p. 576.
3. Jasny, M. *Sounding the Depths. II: The Rising Toll of Sonar, Shipping and Industrial Ocean Noise on Marine Life*; Natural Resource Defence Council: Washington, DC, USA, 2005.
4. National Research Council, NRC. *Marine Mammal Populations and Ocean Noise: Determining When Noise Causes Biologically Significant Effects*; The National Academies Press: Washington, DC, USA, 2005.
5. McDonald, M.A.; Hildebrand, J.A.; Wiggins, S.M. Increases in deep ocean ambient noise in the Northeast Pacific west of San Nicolas Island, California. *J. Acoust. Soc. Am.* **2006**, *120*, 711–718. [CrossRef] [PubMed]
6. McDonald, M.A.; Hildebrand, J.A.; Wiggins, S.M.; Ross, D. A 50-year comparison of ambient ocean noise near San Clemente Island: A bathymetrically complex coastal region off Southern California. *J. Acoust. Soc. Am.* **2008**, *124*, 1985–1992. [CrossRef]
7. Chapman, N.R.; Price, A. Low frequency deep ocean ambient noise trend in the Northeast Pacific Ocean. *J. Acoust. Soc. Am.* **2011**, *129*, EL161–EL165. [CrossRef] [PubMed]
8. Miksis-Olds, J.L.; Nichols, S.M. Is low frequency ocean sound increasing globally? *J. Acoust. Soc. Am.* **2016**, *139*, 501–511. [CrossRef] [PubMed]
9. Andrew, R.K.; Howe, B.M.; Mercer, J.A.; Dzieciuch, M.A. Ocean ambient sound: Comparing the 1960s with the 1990s for a receiver off the California coast. *Acoust. Res. Lett. Online* **2002**, *3*, 65. [CrossRef]
10. Hildebrand, J.A. Anthropogenic and natural sources of ambient noise in the ocean. *Mar. Ecol. Prog. Ser.* **2009**, *395*, 5–20. [CrossRef]
11. Thomsen, F.; McCully, S.R.; Weisse, L.R.; Wood, D.T.; Warr, K.J.; Barry, J.; Law, R.J. Cetacean stock assessments in relation to exploration and production industry activity and other human pressures: Review and data needs. *Aquat. Mam.* **2011**, *37*, 1–93. [CrossRef]
12. Frisk, G.V. Noiseonomics: The relationship between ambient noise levels in the sea and global economic trends. *Sci. Rep.* **2012**, *2*, 1–4. [CrossRef] [PubMed]
13. Merchant, N.D. Underwater noise abatement: Economic factors and policy options. *Environ. Sci. Pol.* **2019**, *92*, 116–123. [CrossRef]
14. Merchant, N.; Brookes, K.; Faulkner, R.; Bicknell, A.W.; Godley, B.J.; Witt, M.J. Underwater noise levels in UK waters. *Sci. Rep.* **2016**, *6*, 36942. [CrossRef] [PubMed]
15. Širović, A.; Evans, K.; Garcia-Soto, C. Trends in inputs of anthropogenic noise into the marine environment. In *UN World Ocean Assessment II*; United Nations Publications: New York, NY, USA, 2021; Chapter 20, Volume II.
16. Hatch, L.T.; Fristrup, K.M. No barrier at the boundaries: Implementing regional frameworks for noise management in protected natural areas. *Mar. Ecol. Prog. Ser.* **2009**, *395*, 223–244. [CrossRef]
17. Williams, R.; Erbe, C.; Ashe, E.; Clark, C.W. Quiet(er) marine protected areas. *Mar. Poll. Bull.* **2015**, *10*, 154–161. [CrossRef] [PubMed]
18. Pirotta, E.; Merchant, N.D.; Thompson, P.M.; Barton, T.R.; Lusseau, D. Quantifying the effect of boat disturbance on bottlenose dolphin foraging. *Biol. Cons.* **2015**, *181*, 82–89. [CrossRef]
19. Cominelli, S.; Devillers, R.; Yurk, H.; MacGillivray, A.; McWhinnie, L.; Canessa, R. Noise exposure from commercial shipping for the southern resident killer whale population. *Mar. Poll. Bull.* **2018**, *136*, 177–200. [CrossRef] [PubMed]
20. National Research Council, NRC. *Ocean Noise and Marine Mammals*; The National Academies Press: Washington, DC, USA, 2003. [CrossRef]
21. Simmonds, M.; Dolman, S.; Weilgart, L. *Oceans of Noise*; A WDCS Science Report WDCS; The Whale and Dolphin Conservation Society: Wiltshire, UK, 2004; p. 168.
22. Weilgart, L.S. The impacts of anthropogenic ocean noise on cetaceans and implications for management. *Can. J. Zool.* **2007**, *85*, 1091–1116. [CrossRef]

23. Southall, B.L.; Bowles, A.E.; Ellison, W.T.; Finneran, J.J.; Gentry, R.L.; Greene, C.R., Jr.; Kastak, D.; Ketten, D.R.; Miller, J.H.; Nachtigall, P.E. Marine mammal noise-exposure criteria: Initial scientific recommendations. *Bioacoust.-Int. J. Anim. Sound Record.* **2007**, *17*, 273–275.
24. Clark, C.W.; Ellison, W.T.; Southall, B.L.; Hatch, L.; Van Parijs, S.M.; Frankel, A.; Ponirakis, D. Acoustic masking in marine ecosystems: Intuitions, analysis, and implication. *Mar. Ecol. Prog. Ser.* **2009**, *395*, 201–222. [CrossRef]
25. Rolland, R.M.; Parks, S.E.; Hunt, K.E.; Castellote, M.; Corkeron, P.J.; Nowacek, D.P.; Wasser, S.K.; Kraus, S.D. Evidence that ship noise increases stress in right whales. *Proc. Royal Soc. B Biol. Sci.* **2012**, *279*, 2363–2368. [CrossRef]
26. Erbe, C.; Reichmuth, C.; Cunningham, K.; Lucke, K.; Dooling, R. Communication masking in marine mammals: A review and research strategy. *Mar. Poll. Bullet.* **2016**, *103*, 15–38. [CrossRef]
27. Wiley, D.; Hatch, L.; Thompson, M.; Schwehr, K.; MacDonald, C. Marine Sanctuaries and Marine Planning: Protecting endangered marine life. *Proc. Mar. Saf. Secur. Counc.* **2013**, *70*, 10–15.
28. Hatch, L.T.; Wahle, C.M.; Gedamke, J.; Harrison, J.; Laws, B.; Moore, S.E.; Van Parijs, S.M. Can you hear me here? Managing acoustic habitat in US waters. *Endanger. Species Res.* **2016**, *30*, 171–186. [CrossRef]
29. Haver, S.M.; Fournet, M.E.H.; Dziak, R.P.; Gabriele, C.; Gedamke, J.; Hatch, L.T.; Haxel, J.; Heppell, S.A.; McKenna, M.F.; Mellinger, D.K.; et al. Comparing the Underwater Soundscapes of Four U.S. National Parks and Marine Sanctuaries. *Front. Mar. Sci.* **2019**, *6*, 500. [CrossRef]
30. Vagle, S.; Neves, M. Evaluation of the effects on underwater noise levels from shifting vessel traffic away from Southern Resident Killer Whale foraging areas in the Strait of Juan de Fuca in 2018. *Can. Tech. Rep. Hydrogr. Ocean Sci.* **2019**, *329*, 6–64.
31. Vagle, S. Evaluation of the efficacy of the Juan de Fuca lateral displacement trial and Swiftsure Bank plus Swanson Channel interim sanctuary zones, 2019. *Can. Tech. Rep. Hydrogr. Ocean Sci.* **2020**, *332*, 6–60.
32. Burnham, R.E.; Vagle, S.; O'Neill, C.; Trounce, K. The Efficacy of Management Measures to Reduce Vessel Noise in Critical Habitat of Southern Resident Killer Whales in the Salish Sea. *Front. Mar. Sci.* **2021**, *8*, 664691. [CrossRef]
33. Payne, R.; Webb, D. Orientation by means of long-range acoustic signaling in baleen whales. *Ann. N. Y. Acad. Sci.* **1971**, *188*, 110–141. [CrossRef]
34. Thompson, T.J.; Winn, H.E.; Perkins, P.J. Mysticete Sounds. In *Behavior of Marine Animals*; Cetaceans, Winn, H.E., Plenum, B.L.O., Eds.; Plenum Press: New York, NY, USA, 1979; Volume 3, pp. 403–431.
35. Watkins, W.A.; Wartzok, D. Sensory biophysics of marine mammals. *Mar. Mamm. Sci.* **1985**, *1*, 219–260. [CrossRef]
36. Clark, C.W. Acoustic behavior of mysticete whales. In *Sensory Abilities of Cetaceans*; Thomas, J.A., Kastelein, R.A., Eds.; Plenum Press: New York, NY, USA, 1990; pp. 571–583.
37. Firestone, J.; Jarvis, C. Response and Responsibility: Regulating Noise Pollution in the Marine Environment. *J. Int. Wild. Law Pol.* **2007**, *10*, 109–152. [CrossRef]
38. Sehgal, A.; Tumar, I.; Schonwalder, J. Effects of climate change and anthropogenic ocean acidification on underwater acoustic communications. In Proceedings of the OCEANS'10 IEEE SYDNEY, Sydney, Australia, 24–27 May 2010; pp. 1–6. [CrossRef]
39. Farina, A. *Soundscape Ecology, Principles, Patterns, Methods and Applications*; Springer Science and Business Media: Dordrecht, The Netherlands, 2014.
40. Medwin, H.; Clay, C.S. *Fundamentals of Acoustical Oceanography*; Academic Press: San Diego, CA, USA, 1998.
41. Southall, B.L.; Finneran, J.J.; Reichmuth, C.; Nachtigall, P.E.; Ketten, D.R.; Bowles, A.E.; Tyack, P.L. Marine mammal noise exposure criteria: Updated scientific recommendations for residual hearing effects. *Aquat. Mamm.* **2019**, *45*, 125–132. [CrossRef]
42. Veirs, S.; Veirs, V.; Wood, J. Ship noise in an urban estuary extends to frequencies used for echolocation by endangered killer whales. *PeerJ PrePrints* **2015**, *3*, e955v3.
43. MacGillivray, A.; Li, Z.; Yurk, H. *Modelling of Cumulative Vessel Noise for Haro Strait Slowdown Trial: Phase 1: Pre-Trial Interim Report*; Version 1.0; Document Number 01443, Technical Report by JASCO Applied Sciences for Vancouver Fraser Port Authority ECHO Program; JASCO Applied Sciences: Victoria, BC, USA, 2017.
44. Gaskin, D.E.; Arnold, P.W.; Blair, B.A. Phocoena phocoena. *Mamm. Species* **1974**, *42*, 1–8.
45. Baird, R.W. *Update COSEWIC Status Report on Harbour Porpoise (Phocoena phocoena) in British Columbia*; Committee on the Status of Endangered Wildlife (COSEWIC): Ottawa, ON, Canada, 2003.
46. Ford, J.K. Killer Whale: Orcinus Orca. In *Encyclopedia of Marine Mammals*; Perrin, W., Wursig, B., Thewissen, J., Eds.; Academic Press: San Diego, CA, USA, 2009; pp. 650–657.
47. Dalla Rosa, L.; Ford, J.K.B.; Trites, A.W. Distribution and relative abundance of humpback whales in relation to environmental variables in coastal British Columbia and adjacent waters. *Cont. Shelf Res.* **2012**, *36*, 89–104. [CrossRef]
48. Department of Fisheries and Oceans Canada, DFO. *Recovery Strategy for the Northern and Southern Resident Killer Whales (Orcinus orca) in Canada*; Species at Risk Act Recovery Strategy Series; Fisheries & Oceans Canada: Ottawa, ON, Canada, 2018; p. x+84.
49. National Oceanic and Atmospheric Administration (NOAA). Endangered and Threatened Species; Designation of Critical Habitat for Southern Resident Killer Whale; 50 CFR Part 226; National Oceanic and Atmospheric Administration (NOAA): National Marine Fisheries Service, Northwest Region, 2006. Available online: https://www.federalregister.gov/documents/2006/11/29/06-9453/endangered-and-threatened-species-designation-of-critical-habitat-for-southern-resident-killer-whale (accessed on 16 September 2021).

50. National Oceanic and Atmospheric Administration (NOAA). *Critical Habitat for the Southern Resident Killer Whales*; National Oceanic and Atmospheric Administration (NOAA): National Marine Fisheries, West Coast Region, 2019. Available online: https://www.fisheries.noaa.gov/action/critical-habitat-southern-resident-killer-whale (accessed on 16 September 2021).
51. Enhancing Cetacean Habitat and Observation (ECHO) Program. *2018 Annual Report*; Enhancing Cetacean Habitat and Observation (ECHO) Program: Vancouver, BC, Canada, 2019; p. 18.
52. Merchant, N.D.; Fristrup, K.M.; Johnson, M.P.; Tyack, P.L.; Witt, M.J.; Blondel, P.; Parks, S. Measuring acoustic habitats. *Methods Ecol. Evol.* **2015**, *6*, 257–265. [CrossRef]
53. Trevorrow, M.V.; Vasiliev, B.; Vagle, S. Directionality and maneuvering effects on a surface ship underwater acoustic signature. *J. Acoust. Soc. Am.* **2008**, *124*, 767–778. [CrossRef]
54. Carey, W.M. Lloyd's Mirror—Image Interference Effects. *Acoust. Today* **2009**, *5*, 14. [CrossRef]
55. Young, R. Image interference in the presence of refraction. *J. Acoust. Soc. Am.* **1947**, *19*, 1–7. [CrossRef]
56. Leroy, C.C.; Robinson, S.P.; Goldsmith, M.J. A New Equation for the Accurate Calculation of Sound Speed in All Oceans. *J. Acoust. Soc. Am.* **2008**, *124*, 2774–2782. [CrossRef]
57. Soontiens, N.; Allen, S.E.; Latornell, D.; Le Souef, K.; Machuca, I.; Paquin, J.-P.; Lu, Y.; Thompson, K.; Korabel, V. Storm surges in the Strait of Georgia simulated with a regional model. *Atmos. Ocean* **2016**, *54*, 1–21. [CrossRef]
58. Soontiens, N.; Allen, S.E. Modelling sensitivities to mixing and advection in a sill-basin estuarine system. *Ocean Model.* **2017**, *112*, 17–32. [CrossRef]
59. Francois, R.; Garrison, G. Sound absorption based on ocean measurements. Part II: Boric acid contribution and equation for total absorption. *J. Acoust. Soc. Am.* **1982**, *72*, 1879–1890. [CrossRef]
60. Bowlin, J.; Spiesberger, J.; Duda, T.; Freitag, L. *Ocean Acoustical Ray Tracing Software RAY*; Technical Report; Woods Hole Oceanographic Institution: Woods Hole, MA, USA, 1992; p. 47.
61. Jensen, F.B.; Kuperman, W.A.; Porter, M.B.; Schmidt, H. *Computational Ocean*; American Institute of Physics: Melville, NY, USA, 1994; p. 634.
62. Hovem, J.M. Ray Trace Modeling of Underwater Sound Propagation. In *Modeling and Measurement Methods for Acoustic Waves and for Acoustic Microdevices*; Beghi, M.G., Ed.; Intech: Rijeka, Croatia, 2013; pp. 573–598.
63. Collins, M.D. A split-step Padé solution for the parabolic equation method. *J. Acoust. Soc. Am.* **1993**, *93*, 1736–1742. [CrossRef]
64. Collins, M.D. An energy-conserving parabolic equation for elastic media. *J. Acoust. Soc. Am.* **1993**, *94*, 975–982. [CrossRef]
65. Hannah, C.G.; Dupont, F.; Collins, A.K.; Dunphy, M.; Greenberg, D. Revisions to a Modelling System for Tides in the Canadian Arctic Archipelago. *Can. Tech. Rep. Hydrogr. Ocean Sci.* **2008**, *259*, 6–62.
66. Williams, T.M.; Davis, R.W.; Fuiman, L.A.; Francis, J.; Le Boeuf, B.J.; Horning, M.; Calambokidis, J.; Croll, D.A. Sink or swim: Strategies for cost-efficient diving by marine mammals. *Science* **2000**, *288*, 133–136. [CrossRef]
67. Goldbogen, J.A.; Calambokidis, J.; Croll, D.A.; Harvey, J.T.; Newton, K.M.; Oleson, E.M.; Schorr, G.; Shadwick, R.E. Foraging behavior of humpback whales: Kinematic and respiratory patterns suggest a high cost for a lunge. *J. Exp. Biol.* **2008**, *211*, 3712–3719. [CrossRef]
68. Doniol-Valcroze, T.; Lesage, V.; Giard, J.; Michaud, R. Optimal foraging theory predicts diving and feeding strategies of the largest marine predator. *Behav. Ecol.* **2011**, *22*, 880–888. [CrossRef]
69. Wright, B.M.; Ford, J.K.; Ellis, G.M.; Deecke, V.B.; Shapiro, A.D.; Battaile, B.C.; Trites, A.W. Fine-scale foraging movements by fish-eating killer whales (*Orcinus orca*) relate to the vertical distributions and escape responses of salmonid prey (*Oncorhynchus* spp.). *Move. Ecol.* **2017**, *5*, 3. [CrossRef]
70. Riera, A.; Pilkington, J.F.; Ford, J.K.B.; Stredulinsky, E.H.; Chapman, N.R. Passive acoustic monitoring off Vancouver Island reveals extensive use by at-risk resident killer whale (*Orcinus orca*) populations. *Endang. Spec. Res.* **2019**, *39*, 221–234. [CrossRef]
71. Tennessen, J.B.; Holt, M.M.; Hansen, M.B.; Emmons, C.K.; Giles, D.A.; Hogan, J.T. Kinematic signatures of prey capture from archival tags reveal sex differences in killer whale foraging activity. *J. Exp. Biol.* **2019**, *222*, 1–13. [CrossRef]
72. Au, W.W.L.; Hastings, M.C. *Principles of Marine Bioacoustics*; Springer Science & Business Media: New York, NY, USA, 2008; p. 680.
73. Haggarty, D.; Gregr, E.; Lessard, J.; Fields Co Davies, S. *Deep Substrate (100 m) for the Pacific Canadian Shelf*; Fisheries and Oceans Canada: Nanaimo, BC, Canada, 2018. Available online: https://www.gis-hub.ca/dataset/substrate100m-data (accessed on 1 April 2021).
74. Mullan, S. Tidal Sedimentology and Geomorphology in the Central Salish Sea Straits, British Columbia and Washington State. Ph.D. Thesis, University of British Columbia, Vancouver, BC, Canada, 2010.
75. Frey, S.E.; Dashtgard, S. Sedimentology, ichnology and hydrodynamics of strait-margin, sand and gravel beaches and shorefaces: Juan de Fuca Strait, British Columbia, Canada. *Sedimentology* **2011**, *58*, 1326–1346. [CrossRef]
76. Hamilton, E.L. Geoacoustic modeling of the sea floor. *J. Acoust. Soc. Am.* **1976**, *68*, 1313–1340. [CrossRef]
77. Hamilton, E.L. Compressional Waves in marine sediments. *Geophysics* **1982**, *37*, 620–646. [CrossRef]
78. Department of Fisheries and Oceans Canada, DFO. *Evaluation of the Scientific Evidence to Inform the Probability of Effectiveness of Mitigation Measures in Reducing Shipping-Related Noise Levels by Southern Resident Killer Whales*; Department of Fisheries and Oceans Canada, DFO: Ottawa, ON, Canada, 2017; DFO Can. Sci. Advis. Sec. Sci. Advis. Rep. 2017; 2017/041.
79. Lacy, R.C.; Williams, R.; Ashe, E.; Balcomb, K.C., III; Brent, L.J.N.; Clark, C.W.; Croft, D.P.; Giles, D.A.; MacDuffee, M.; Paquet, P.C. Evaluating anthropogenic threats to endangered killer whales to inform effective recovery plans. *Sci. Rep.* **2017**, *7*, 14119. [CrossRef] [PubMed]

80. Pirotta, V.; Grech, A.; Jonsen, I.D.; Laurance, W.F.; Harcourt, R.G. Consequences of global shipping traffic for marine giants. *Front. Ecol. Environ.* **2019**, *17*, 39–47. [CrossRef]
81. Miller, P.J. Diversity in sound pressure levels and estimated active space of resident killer whale vocalizations. *J. Comp. Physiol. A* **2006**, *192*, 449–459. [CrossRef]
82. Holt, M.M.; Noren, D.P.; Emmons, C.K. Effects of noise levels and call types on the source levels of killer whale calls. *J. Acoust. Soc. Am.* **2011**, *130*, 3100–3106. [CrossRef]
83. Heise, K.A.; Barrett-Lennard, L.G.; Chapman, N.R.; Dakin, D.T.; Erbe, C.; Hannay, D.E.; Merchant, N.D.; Pilkington, J.S.; Thornton, S.J.; Tollit, D.J.; et al. *Proposed Metrics for the Management of Underwater Noise for Southern Resident Killer Whales*; Coastal Ocean Report Series (2); Ocean Wise: Vancouver, BC, Canada, 2017; p. 30.
84. Bigg, M.A.; Olesiuk, P.F.; Ellis, G.M.; Ford, J.K.B.; Balcomb, K.C. *Social Organization and Genealogy of Resident Killer Whales (Orcinus Orca) in the Coastal Waters of British Columbia and Washington State*; Report of the International Whaling Commission; The International Whaling Commission: Cambridge, UK, 1990; Volume 12, pp. 383–405.
85. Hertel, H. *Structure, Form, Movement*; Reinhold Publishing Company: New York, NY, USA, 1966.
86. Baird, R.W.; Hanson, M.B.; Dill, L.M. Factors influencing the diving behaviour of fish-eating killer whales: Sex differences and diel and interannual variation in diving rates. *Can. J. Zool.* **2005**, *83*, 257–267. [CrossRef]
87. Audoly, C.; Rousset, C.; Folegot, T.; Andre, M.; Benedetti, L.; Baudin, E.; Salinas, R. AQUO Project 'Achieve quieter oceans by shipping noise footprint reduction'. In Proceedings of the 3rd International Conference on Advanced Model Measurement Technology for the EU Maritime Industry, Gdansk, Poland, 17–18 September 2013.
88. MacGillivray, A.O.; Li, Z.; Hannay, D.E.; Trounce, K.B.; Robinson, O. Slowing deep-sea commercial vessels reduces underwater radiated noise. *J. Acoust. Soc. Am.* **2019**, *146*, 340–351. [CrossRef] [PubMed]
89. Thomson, D.J.M.; Barclay, D.R. Real-time observations of the impact of COVID-19 on underwater noise. *J. Acoust. Soc. Am.* **2020**, *147*, 3390. [CrossRef]
90. Dransfield, A.; Hines, E.; McGowan, J.; Holzman, B.; Nur, N.; Elliott, M.; Howar, J.; Jahncke, J. Where the whales are: Using habitat modeling to support changes in shipping regulations within National Marine Sanctuaries in Central California. *Endanger. Species Res.* **2014**, *26*, 39–57. [CrossRef]
91. McGregor, P.K.; Horn, A.G.; Leonard, M.L.; Thomsen, F. Anthropogenic noise and Conservation. In *Animal Communication and Noise*; Brumm, H., Ed.; Springer: Berlin/Heidelberg, Germany, 2013; pp. 409–444.
92. Ruser, A.; Dähne, M.; van Neer, A.; Lucke, K.; Sundermeyer, J.; Siebert, U.; Teilmann, J. Assessing auditory evoked potentials of wild harbor porpoises (*Phocoena phocoena*). *J. Acoust. Soc. Am.* **2016**, *140*, 442–452. [CrossRef] [PubMed]
93. Mooney, T.A.; Castellote, M.; Quakenbush, L.; Hobbs, R.; Gaglione, E.; Goertz, C. Variation in hearing within a wild population of beluga whales (*Delphinapterus leucas*). *J. Exp. Biol.* **2018**, *221*, jeb171959. [CrossRef] [PubMed]
94. Burnham, R.E.; Vagle, S.; O'Neill, C. Spatiotemporal patterns in the natural and anthropogenic additions to the soundscape in parts of the Salish Sea, British Columbia, 2018–2020. *Mar. Poll. Bull.* **2021**, *170*, 112647. [CrossRef]
95. Council of Canadian Academies, CCA. *The Value of Commercial Marine Shipping to Canada*; The Expert Panel on the Social and Economic Value of Marine Shipping to Canada, Council of Canadian Academies: Ottawa, ON, Canada, 2017.